

Simultaneous Analysis of the UV Curing of Acrylate-Nanoparticle Formulations by Combined Photorheometry and FT-NIR Spectroscopy

Tom Scherzer^{}, Martin W. Schröder*

Leibniz Institute of Surface Modification (IOM), Leipzig, Germany

Introduction

UV curing reactions typically proceed within fraction of a second. This makes it difficult to analyze network formation and the corresponding physical and chemical changes in the sample during the reaction. In the past, various methods have been used to follow the chemical changes, in particular the conversion of the functional groups. Photo-DSC [1] and real-time FTIR spectroscopy [2,3] have been applied to study the chemical kinetics of the curing reaction. For monitoring of the rapid changes of the viscoelastic and mechanical properties, photorheometry has been developed [4-6]. This method allows one to detect, for instance, the occurrence of structural transitions such as gelation and vitrification. However, it cannot provide information, which is necessary for understanding the chemical mechanisms during curing (e.g. conversion). The combination of both spectroscopic and rheometric data may overcome this problem. However, it is usually difficult to compare gelation and vitrification times with the conversion because two different experiments have to be carried out: one for the measurements of gelation and vitrification times and another one for the monitoring of the conversion.

For this reason, a more sophisticated method has been proposed [7,8]: the coupling of photorheometry with vibrational spectroscopy allows one to monitor both the viscoelastic properties and the extent of the conversion simultaneously, e.g. in one experiment. Near-infrared (NIR) spectroscopy is preferred to FTIR spectroscopy in the mid-infrared for various reasons such as thickness limitations in FTIR spectroscopy and the availability of optical fibers in the NIR range. The most important problem is the spatial arrangement of UV irradiation and NIR measurement in the rheological device. Various approaches have been proposed in the past. Details also depend on the type of rheometer used, i.e. if the stress is transmitted to the sample by the upper or the lower plate. Several authors reported the replacement of the upper (immobile) plate of the rheometer by a quartz plate. Moreover, the plate holder was replaced by a tube, which allows UV illumination through the tube [5,7,8]. NIR spectra were measured either in transmission by passing the probe beam through the edges [9] or transversely through the center of the quartz plates [8], respectively, or in transflection mode [7].

Another approach will be demonstrated in the present study. The (immobile) lower plate of the rheometer was replaced by a quartz plate. This allows both UV irradiation and NIR measurement from the bottom up. NIR spectra were measured in transflection mode using the top plate of the rheometer as reflector for the probe beam.

Experimental

Dynamic mechanical analysis (DMA) was carried out with a Physica MCR 300 rheometer (Anton Paar). For photopolymerization studies, it was equipped with a UV cell. In this cell, the lower plate of the conventional plate-to-plate measuring system is replaced by a quartz plate, which allows UV irradiation of the sample. Moreover, the temperature of the sample is controlled by both Peltier heating (or cooling) of the quartz plate and convection heating of the environmental chamber (up to 120°C). In the present study, a disposable aluminium plate with a diameter of 10 mm was used as upper tool in order to be able to record strain data during the complete experiment.

* e-mail: tom.scherzer@iom-leipzig.de

UV radiation was supplied by a Hamamatsu LC-5 UV spot light source (200 W HgXe bulb, optical bandpass filter 300...400 nm), which is linked to the rheometer by a light guide (diameter 3 mm). The end of the fiber is fixed 30 mm below the center of the quartz plate, which allows homogeneous irradiation of the complete area below the top plate. A scheme of the setup is shown in Fig. 1. The intensity of the UV radiation at the sample position can be varied between 8 and 60 mW cm⁻². In the present study, it was set to 10 mW cm⁻². Irradiation was carried out under inert conditions by flushing the environmental chamber with nitrogen.

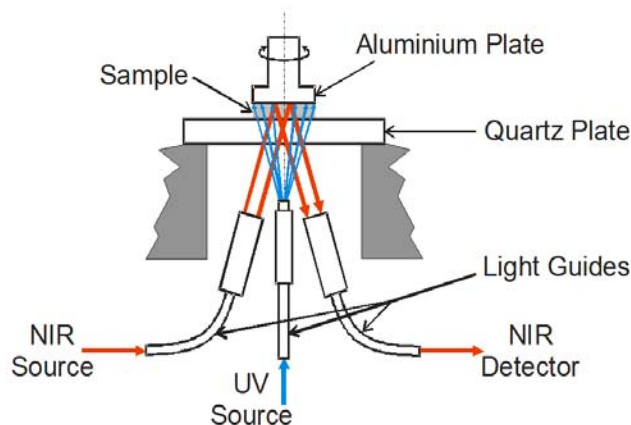


Fig. 1: Scheme of the experimental setup

For the spectroscopic measurements, a Bruker Multi Purpose Analyzer (MPA) FT-NIR spectrometer was used, which is equipped with a tungsten halogen light source, a quartz beam splitter and a thermoelectrically cooled InGaAs detector. By use of the chromatography module CHROM of the OPUS software package, NIR spectra can be recorded in real time. At a spectral resolution of 32 cm⁻¹, a sampling rate of 8.5 spectra s⁻¹ was achieved.

The NIR spectrometer is linked to the rheometer by two optical quartz fibers (length 1 m, diameter 600 μm), which are equipped with collimating lenses (diameter 6 mm, Hellma). The fibers ends are fixed below the quartz plate (see Fig. 1). The NIR beam is directed towards the aluminium plate, i.e. the upper tool of the measuring system. After reflection at this plate, the probe light is collected by the collimator of the other fiber.

Synchronization between the DMA measurement, NIR spectroscopy and UV irradiation is achieved by triggering the start of the collection of NIR spectra as well as the opening of the shutter of the UV lamp by the rheometer software. The experiments were subdivided into several phases with different experimental conditions. In the first step, the state of the sample before UV curing was analyzed. DMA and NIR data acquisition started simultaneously. A sinusoidal strain of 10 % with a frequency of 20 Hz was applied to the sample, and DMA data were recorded at a rate of one value per second. In the second step, UV illumination of the sample started. The applied strain was decreased from 10 % to 0.05 % using a logarithmical ramp and a sampling rate of 10 s⁻¹. This ramping of the applied strain is necessary because of the strong change of the modulus of the sample during network formation. If the strain would not be reduced, the maximum allowable torque of the instrument would be exceeded. Moreover, the decrease of the strain makes sure that the deformation of the sample remains in the linear viscoelastic (LVE) range. Later, the DMA sampling rate was reduced to 1 s⁻¹ and then to 0.1 s⁻¹. Finally, the UV illumination was stopped while DMA and NIR data were still recorded for 3.5 min. During the measurement, the automatic gap control of the rheometer was activated, which compensates for changes of the thickness due to the shrinkage of the sample during polymerization. The extent of shrinking can be estimated from the relation between the actual gap and the gap before the reaction. The initial thickness of the sample was 400 μm.

The dynamic shear modulus G^* was calculated by taking the ratio of the stress and strain amplitude, while the phase angle $\tan \delta$ was obtained from the phase shift between these two signals.

The extent of conversion can be directly obtained from the decrease of the absorption band at 6170 cm⁻¹, which is assigned to the first overtone of the C-H stretching vibration of the acrylic double bond.

Samples

Methacryl-grafted silica nanoparticles were prepared according to Ref. [10]. The silica nanopowder (Aerosil OX50, mean particle size 40 nm) was intensively stirred in boiling acetone. Methacroyloxypropyltrimethoxysilane (DYNASYLAN MEMO) and maleic anhydride diluted in water were added. This mixture was refluxed for 2 h. The resulting modified nanopowder was dried under vacuum. Then, the nanoparticles were dispersed into a mixture of a bisphenol A epoxy diacrylate oligomer (CN 104, Sartomer, 2 parts) and tripropylene glycole diacrylate (TPGDA, 1 part). Formulations with different amounts of nanoparticles, i.e. with 0, 5, 10, 15, 20, 25, and 30 %, were prepared. Lucirin TPO-L was added at a concentration of 0.5 % relative to the binder formulation. Finally, the mixture was sonicated for homogenization and in order to remove air bubbles.

Effect of Temperature on the UV Curing of Acrylate / Nanoparticle Formulations

Temperature is well-known to have a strong influence on the kinetics of UV curing reactions. In the past, its effect has been studied by photo-DSC [11] and real-time FTIR-spectroscopy [12]. It has been shown that the effect of temperature is mainly due to the decrease of the viscosity of the formulation [12]. In the present study, the viscoelastic behavior of acrylate / nanoparticle formulations as well the kinetics of the conversion of the double bonds was followed simultaneously by combined photorheometry and NIR spectroscopy.

From dynamic mechanical analysis, the complex viscosity η^* can be determined. Fig. 2 shows the viscosity of the uncured and unmodified formulation, which strongly depends on temperature as expected.

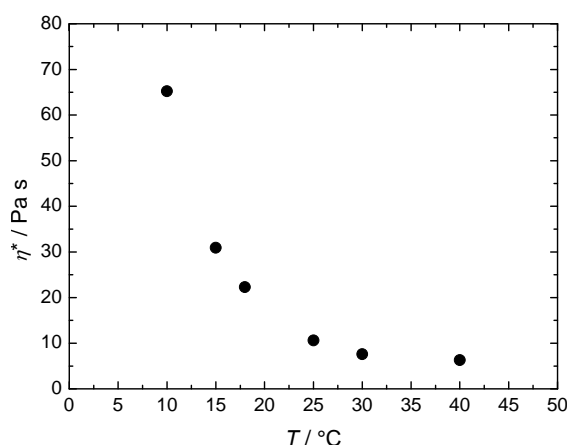


Fig. 2: Complex viscosity η^* of the uncured samples as function of the sample temperature.

The evolution of the complex shear modulus upon UV irradiation at various temperatures from 10°C to 40°C is shown in Fig. 3. The complex shear modulus represents the viscoelastic properties of the sample. After opening of the shutter, the UV-induced initiation leads to radical polymerization and to the buildup of a cross-linked polymer network. Cross-linking transforms the initially liquid formulation into a solid polymer, which is usually vitreous. This transformation is reflected by a strong increase of the shear modulus by up to 9 orders of magnitude. The slopes of the curves strongly depend on the temperature during polymerization. The initial slope of the complex shear modulus curve increases with increasing temperature, which reflects a faster buildup of the network due to a faster curing reaction. However, the shear modulus of samples cured at higher temperatures tends to level off soon, whereas it further increases for samples cured at lower temperatures. This behavior is related to (i) the higher conversion achieved in the former samples and (ii) the decreasing difference of the curing temperature to the glass temperature. Therefore, the shear modulus was measured again for all samples after cooling down or heating up, respectively, to 25°C. It is apparent that the order of the samples reversed: the higher the temperature, at which the sample was cured (e.g. the higher the conversion), the higher is the module at room temperature.

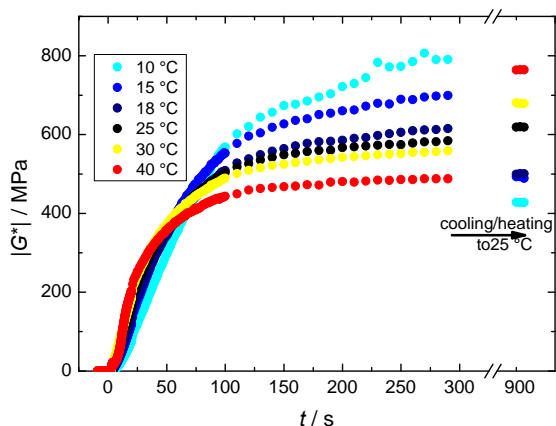


Fig. 3: Evolution of the complex shear modulus $|G^*|$ as function of time at various temperatures.

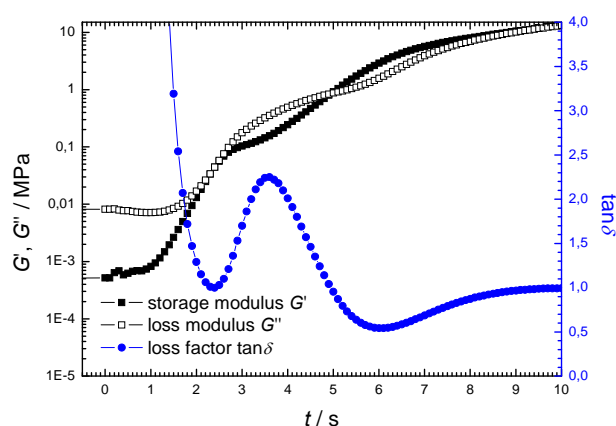


Fig. 4: Storage modulus G' , loss modulus G'' and loss factor $\tan\delta$ as a function of time.

The initial phase of the reaction is shown in detail in Fig. 4. In particular, the curves of the storage (G') and the loss (G'') modulus as well as the loss factor $\tan\delta = G''/G'$ are given. The loss factor represents the relation between the viscous and the elastic part of the shear modulus. It varies from infinite in the liquid state to a value close zero in the vitreous state.

Gelation corresponds to the transition from a viscous liquid to an elastic solid. Two criteria are generally used to determine the occurrence of gelation: the crossover of the storage and the loss moduli, which corresponds to $\tan\delta = 1$, or the point, at which the loss factor becomes independent of frequency. Moreover, the criterion $\eta' = 1000 \text{ Pa s}$ has been proposed [13]. Accordingly, the acrylate formulation was found to gel after about 2.5 s upon irradiation at 10°C (Fig. 4). For the detection of vitrification, the occurrence of a peak in the curve of $\tan\delta$ vs. time was used as criterion [14]. This peak can be clearly observed in Fig. 4: the sample passes into the glassy state after about 3.6 s. Vitrification is a gradual process, which occurs over a wide conversion range. This phenomenon is reflected by the rather broad peak.

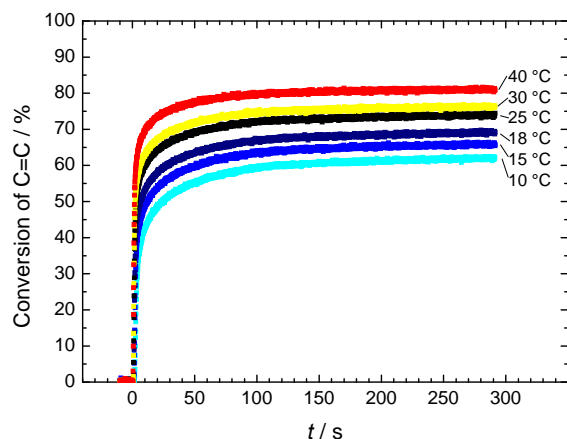


Fig. 5: Temperature dependence of the conversion of the acrylate double bonds

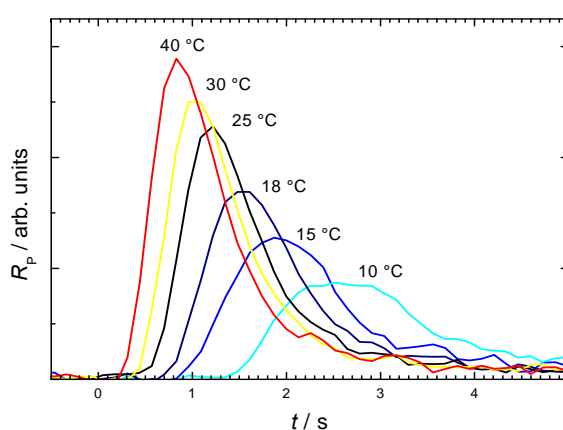


Fig. 6: Temperature dependence of the polymerization rate R_p

The strong influence of temperature on the kinetics of the UV-induced polymerization reaction and the resulting conversion of the acrylate double bonds is shown in Fig. 5. The higher the temperature of the sample, the faster the curing reaction becomes, which clearly correlates with the results in Fig. 3. The observed value of double bond conversion at the end of the measurement also depends on temperature. Predictably, it strongly increases with increasing temperature. From the curves in Fig. 5, the polymerization rates were determined. Results are given in Fig 6. According to the Arrhenius law, the maximum polymerization rate at 40°C is about 3.3 times higher than at 10°C. Moreover, the time of the occurrence of the maximum polymerization rate is shifted from 0.8 s at 40°C to 2.7 s at 10°C.

It is well-known that the maximum in the curve of the polymerization rate $R_{p,max}$ corresponds to the gel point. The development of a continuous network strongly limits the mobility of the functional groups, which leads to a sharp decrease of the reaction rate. Consequently, the time to achieve $R_{p,max}$ has to be in accordance with the gelation time t_{gel} . Fig. 7 compares the values of t_{gel} determined by rheometry with $t_{R_{p,max}}$ extracted from spectroscopic data. It is apparent that both data sets show excellent correlation. The slight deviation at 10°C obviously reflects the broad peak in the curve of the polymerization rate.

The major advantage of the coupling of photorheometry and NIR spectroscopy is the ability to characterize the evolution of the modulus in dependence on the conversion, which were both measured simultaneously in one single experiment. In Fig. 8, the complex shear modulus is plotted in dependence on the acrylate conversion. With increasing temperature, $|G^*|$ starts to increase at higher and higher conversion, which is due to the fact that the system remains softer at higher temperatures.

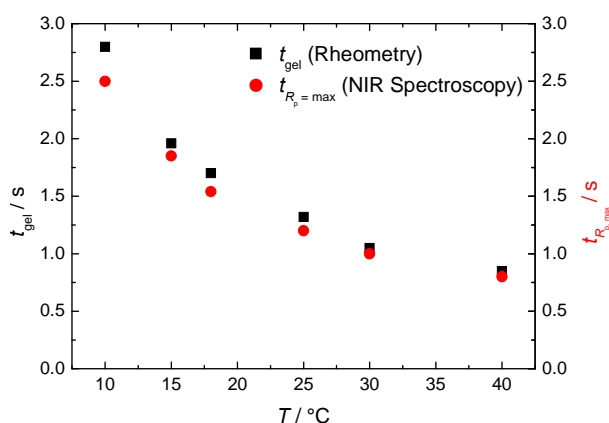


Fig. 7: Gelation times (t_{gel}) and times to achieve maximum polymerization rate ($t_{R_{p,max}}$) at various temperatures.

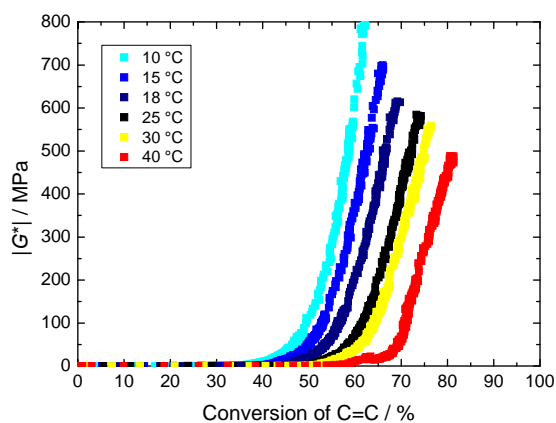


Fig. 8: Complex shear modulus $|G^*|$ as function of the conversion of acrylic double bonds.

Effect of the Concentration of Nanoparticles

The mechanical properties of polymeric nanocomposites do not only depend on the chemistry of the nanoparticles used for modification but also on their content in the polymer matrix. However, in case of the use of such nanocomposites in UV-curable coatings it has to be considered if the increasing content of nanoparticles influences the curing kinetics of the formulations. Photorheometry in combination with NIR spectroscopy is an excellent tool for such studies.

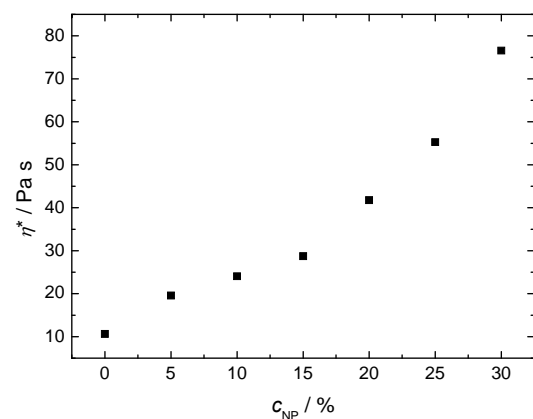


Fig. 9: Complex viscosity η^* of the uncured samples at 25°C as function of the concentration of nanoparticles

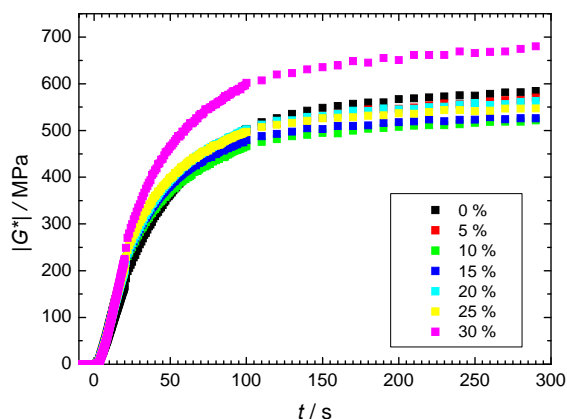


Fig. 10: Evolution of the complex shear modulus $|G^*|$ as function of time and the concentration of nanoparticles

The viscosity of the modified formulations strongly depends on the nanoparticle concentration, which is shown in Fig. 9. With increasing filler content the viscosity increases exponentially. So, the viscosity of the formulation with the highest particle concentration (30 %) is about 8 times higher than that of the pure binder formulation.

Fig. 10 shows the effect of the content of methacroyl-grafted silica nanoparticles in the formulation based on an epoxy acrylate on the evolution of the complex shear modulus. It is obvious that there is only little influence on the mechanical parameters at nanoparticle concentrations up to about 25 %. Only the sample containing 30 % nanoparticles shows a significant increase of the modulus. This result is in accordance with previous findings [15-17], which have shown that a minimum of 30 % nanoparticles is required for substantial improvements of the mechanical resistance.

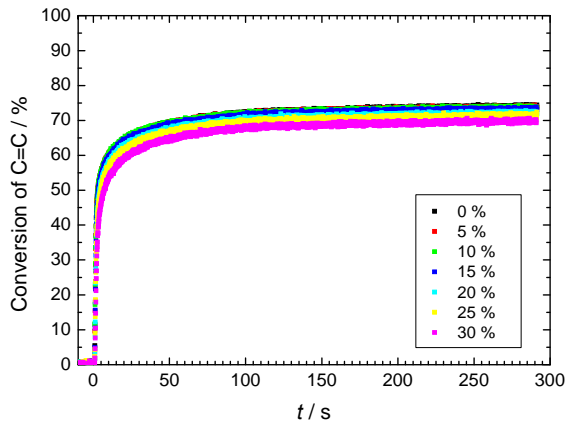


Fig. 11: Effect of the nanoparticle concentration on the kinetics of the UV-induced curing process.

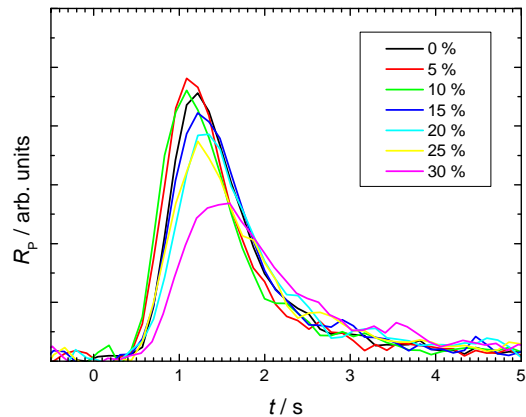


Fig. 12: Effect of the nanoparticle concentration on the polymerization rate R_p .

Similar results were also obtained for the kinetics of the photopolymerization reaction. The development of the conversion of the acrylic double bonds in formulations containing various amounts of nanoparticles is shown in Fig. 11. The corresponding curves of polymerization rate are given in Fig. 12. Evidently, the curing kinetics does not depend on the degree of modification up to a nanoparticle concentration of 25 %. This is in accordance with the excellent transmission of these systems, i.e. the incident UV light can deeply penetrate into the coatings and initiate the curing reaction, which leads to homogeneous through cure of the coatings. Only at 30 % modified silica, a slight effect on the polymerization rate is observed.

Correspondingly, the gelation times and the times to achieve maximum polymerization rate are largely independent of the nanoparticles content as well (see Fig. 13).

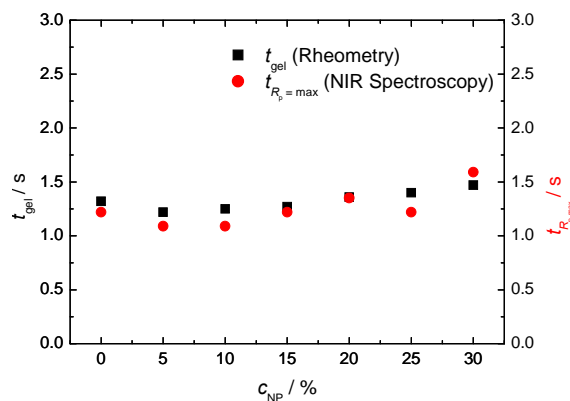


Fig. 13: Gelation times (t_{gel}) and times to achieve maximum polymerization rate ($t_{R_p,max}$).

Conclusion

In this study, a new experimental setup for the coupling of photorheometry and NIR spectroscopy was introduced. This method proved to be a powerful analytical tool for the investigation of UV photopolymerization reactions. It allows simultaneous and time-resolved monitoring of both the chemical conversion and various viscoelastic parameters (e.g. viscosity, shear modulus), i.e. the evolving rheological properties can be followed in dependence on the actual conversion. In the present work, the combined method was applied to the investigation of the curing process of acrylate formulations, which were modified with nanoparticles. The effects of the temperature during curing and the concentration of nanoparticles in the formulations were studied. In particular, gelation and vitrification times from rheometry were compared with the times to reach maximum polymerization rate determined from the spectroscopic data. Excellent correlation between both parameters was observed.

Acknowledgements

The authors would like to thank Stefanie Kriehn and Sören Pyczak for technical assistance. Financial support was kindly provided by the AiF association under grant number 15354 BG.

References

- [1] J.E. Moore, in: S.P. Pappas SP, ed., *UV Curing: Science and Technology*, Technology Market Publishers, Stanford, 1978. p. 133.
- [2] C. Decker, K. Moussa, *Makromol.Chem.* **189**, 2381 (1989).
- [3] T. Scherzer, U. Decker, *Vibr. Spectrosc.* **19**, 385 (1999).
- [4] S.A. Khan, I.M.Plitz, R.A. Frantz, *Rheol. Acta* **31**, 151 (1992).
- [5] L.E. Schmidt, Y. Leterrier, J.M. Vesin, M. Wilhelm, J.A.E. Månson, *Macromol. Mater. Engin.* **290**, 1115 (2005).
- [6] J. Schall, A.F. Jacobine, J.G. Woods, R.N. Coffey, *Proc. RadTech Europe Conf. 2007*, Vienna, 13.-15.11.2007.
- [7] P.A.M. Steeman, A.A. Dias, D.Wenke, T. Zwartkruis, *Macromolecules* **37**, 7001 (2004).
- [8] A. Botella, J. Dupuy, A.A. Roche, H. Sautereau, V. Verney, *Macromol. Rap. Comm.* **25**, 1155 (2004).
- [9] S. Benali, J. Bouchet, G. Lachenal, *J. Near Infrared Spectros.* **12**, 5 (2005).
- [10] F. Bauer, H. Ernst, U. Decker, M. Findeisen, H.-J. Gläsel, H. Langguth, E. Hartmann, R. Mehnert, C. Peuker, *Macromol. Chem. Phys.* **201**, 2654 (2000).
- [11] D.J. Broer, G.N. Mol, G.N. Challa, *Polymer* **32**, 690 (1991).
- [12] T. Scherzer, U. Decker, *Polymer* **41**, 7681 (2000).
- [13] C. Pillot, J. Guillet, J.P. Pascault, *Angew. Makromol. Chem.* **81**, 35 (1979).
- [14] J. Lange, N. Altmann, C.T. Kelly, P.J. Halley, *Polymer* **41**, 5949 (2000).
- [15] H.-J. Gläsel, F. Bauer, H. Ernst, M. Findeisen, E. Hartmann, H. Langguth, R. Mehnert, R. Schubert, *Macromol. Chem. Phys.* **201**, 2765 (2000).
- [16] F. Bauer, H.-J. Gläsel, U. Decker, H. Ernst, A. Freyer, E. Hartmann, V. Sauerland, R. Mehnert, *Progr. Org. Coat.* **47**, 147 (2003).
- [17] K. Heymann, G. Mirschel, S. Kriehn, S. Polage, T. Scherzer, unpublished results.